DYNAMICS OF DROP COALESCENCE ON A SURFACE: THE ROLE OF INITIAL CONDITIONS AND SURFACE PROPERTIES[1]

R. Narhe, D. Beysens[2] and V. Nikolayev
ESEME, SBT, CEA-Grenoble, Grenoble (France)
Mailing address: CEA-ESEME, ICMCB, 87, Av. Dr. A. Schweitzer, 33608
Pessac Cedex (France)
email: narhe@icmcb.u-bordeaux.fr ; dbeysens@cea.fr

Abstract

We present here investigation of the coalescence of two water drops on a surface and compare with spreading. The associated capillary numbers are very low ($< 10^{-5}$). The drops relax exponentially towards equilibrium. The typical relaxation time increases with decreasing contact angle as proposed by Nikolayev and Beysens [1] following a non-local approach. This time is proportional to the drop radius, thus defining a velocity U. The corresponding U values are smaller by many order of magnitude than the bulk hydrodynamic velocity (σ/η, with σ the gas-liquid surface tension and η the viscosity).

We find that the dynamics of receding (coalescence) and spreading motion is of the same order when coalescence or spreading is induced by a syringe. However, dynamics is systematically faster by an order of magnitude when comparing syringe deposition with condensation induced coalescence. We explain this fast dynamics by looking at the initial coalescence stage with a fast camera. The composite drop is initially vigorously excited by deformation modes, favoring contact line motion, a phenomenon that is not observed with condensation-induced coalescence. The dynamics is also faster for rough substrate, as the contact line is soon pined on defects in a metastable state.

Keywords: contact angle, coalescence, capillary force, contact line velocity, hydrodynamic velocity, spreading

---

[1]Paper presented at the Fifteenth Symposium on Thermophysical Properties, June 22-27,2003 Boulder, Colorado, U.S.A

[2]To whom correspondence should be addressed. E-mail: dbeysens@cea.fr

1. INTRODUCTION

In number of industrial and material processing the coalescence of drops plays an important role; for instance liquid mixtures, polymers, sintering of alloys etc. Apart from this, the drop spreading or coalesceing has attracted a number of scientists and is a very active field of research. The dynamics of the three-phase contact line is very sensitive to a number of factors e.g. chemical/geometrical defects, presence of liquid film on solid surface, the wetting properties of substrate itself etc.

The dynamics of liquid spreading have been studied extensively. The hydrodynamic model of de Gennes [2] described the spreading of liquid in presence of a precursor film. This precursor film facilitates the spreading. However, it was clearly observed in ellipsometric and molecular dynamics study [3,4] of spreading of drops that the precursor film is absent in case of partial wetting. The theory proposed by of Blake and Haynes [5] considered molecular displacement of atoms of spreading liquid occurring randomly in vicinity of advancing contact line. Pomeau [6] has explained the dynamics of contact line by taking into account a phase transition. Almost all the models have agreed on a general relationship between normal component of contact line velocity v_n and the dynamic contact angle θ of form

$$v_{n=} \frac{\sigma}{\xi}\left(cos\,\theta_{eq} - cos\,\theta\right) \qquad (1)$$

where σ is interfacial surface tension, ξ model dependent dissipation coefficient, θ_{eq} is equilibrium contact angle. Also all these models predict a large ξ value with respect to the shear viscosity η, so $K = \eta/\xi$ is small.

In studies of contact line dynamics the relation (1) was considered universal for a long time. Recently, Nikolayev and Beysens [1] have developed a non-local dynamic approach and applied it to the analysis of the relaxation of the composite drop formed by the coalescence of two drops. They showed that for a case where v_n varies along the contact line eq. (1) is not valid

The purpose of the present work is (1) to extend the study of Andrieu et al. [7] and (ii) to investigate several different ways to initiate the coalescence of the drops, essentially condensation growth and syringe deposition, thus evaluating the impact of the initial conditions on the dynamics of coalescence and spreading.

2. EXPERIMENTAL

For this study silicon wafers (untreated and treated) and polyethylene sheets ($\approx$ 50 μm thick) were used as substrates with different average contact angle and hysteresis. The coalescence of two drops is studied either in (i) a condensation chamber (chamber experiments, CE), where droplets grow by condensation and coalesce when they touch each other, and (ii) by adding a small drop on top of two neighboring drops (syringe experiments, SE). This method also enables (iii) spreading of one drop to be studied.

2.1. Chamber experiments:

The setup for the condensation experiment is typical for studying breath figures and has been already described in [7]. Here we only outline some basic features. The condensation assembly consists of a Peltier-element thermostat (to lower the substrate temperature) in a closed Plexiglas chamber. Nitrogen gas saturated with water at room

temperature (23°C) is sent into to the chamber with fixed flow rate (0.6 l/min). The experimental procedure consists of cooling the substrate down to the desired temperature and sending N_2 saturated with water vapor into the chamber. The growth of condensation pattern is observed by an optical microscope and recorded by a CCD camera on videotapes. The video data are then analyzed by image processing system.

2.2 Syringe experiments

In syringe experiments two small water drops of known volume were deposited very close to each other on a substrate. In order to induce coalescence, a small drop is deposited on the top of one of the drops. The process of coalescence and relaxation was filmed with CCD camera equipped with a macrozoom lens and recorded on video recorder. The initial process of fusion of two drops for both chamber and syringe experiments was observed with a high speed CCD camera (HCC1000 strobe,1000 frames/s). For the spreading study, a small water drop of known volume was deposited from a distance of 2-3 mm on the substrate. The syringe experiments were all performed at open room atmosphere (room temperature and humidity). In order to test a possible temperature and humidity dependence, the syringe experiments were carried out at different temperatures of the substrate T_s such that $T_s > T_D$, $T_s = T_D$, $T_s = T_D - 5K$, where T_D denotes the dew temperature. We observed that the change in temperature does not affect the relaxation of the composite drop. When $T_s < T_D$, tiny condensing drops are visible on the substrate, some of them coalesce with the composite drop formed during the coalescence of two deposited drops. The volume change of the composite drop due to these multiple coalescence is negligible and the triple line motion is not affected.

2.3 Surface properties

The following substrates were used: (i) 50 μm thick polyethylene sheet, (ii) silicon wafers with different surface treatment. The surface properties, which determine the contact angle, are changed on silicon surface using the silanization procedure as described in [8]. However, in our case the substrate was kept above the cavity containing decyltrichlorosilane. The contact angle is changed by varying the distance between the substrate and the cavity while silanization time was kept fixed (1min). The contact angle of water on a substrate is measured by the sessile drop method. A small drop of 1 μl is deposited on the substrate by means of a microliter syringe and visualized using the CCD camera with a macro lens. The receding contact angle (θ_r) and advancing contact angle (θ_a) are measured by adding/removing with the microsyringe a small amount of water to/from the drop. The value of θ_a and θ_r for silicon and polyethylene substrates are given in Table I. Under θ_{eq} we mean that $(\theta_a + \theta_r)/2$.

3. RESULTS AND DISCUSSION

3.1. Coalescence in condensation chamber

We confirm and extend the data obtained by Andrieu et al.[7]. Fig. 1 shows typical microscopic pictures of the coalescence of two hemispherical drops in the condensation chamber. A new composite elongated drop is formed. Its shape can be characterized by the large axis 2Ry measured in the direction of the elongation and the small axis 2Rx measured in the perpendicular direction. The large and small drop radii Ry and Rx are defined as half of the corresponding axis. The composite drop finally

becomes hemispherical with equilibrium radius R. The dynamics is very slow and the complete relaxation takes a long time. The relaxation velocity is proportional to the restoring force F which is defined by the change of the drop energy, i.e. drop free surface area, see Nikolayev and Beysens [1]. The coalescence process is characterized by three time stages as observed by Andrieu et al.[7]. 1) Formation of liquid bridge, 2) Decrease of large radius Ry and increase of small radius Rx such that the ratio Ry/Rx eventually reaches a value about unity, and 3) Slow growth due to condensation. Fig 2 shows the time evolution of large radius R_y and small radius R_x of the composite drop.

On the stage 2 the restoring force F can be approximated by the expression

$$F = 2\pi R \sigma_{lv} \left(\cos\theta - \cos\theta_r \right) \tag{2}$$

where $\theta = \theta(t)$ is the time dependent dynamic receding contact angle at the points M_1 and M_2 that lie on the long axis. The expression (2) is exact for the spherical cap shape [9]. A rough evaluation of the initial value of this force per unit length

$$f = \frac{F}{2\pi R} = \sigma_{lv} \left(\cos\theta_0 - \cos\theta_r \right) \tag{3}$$

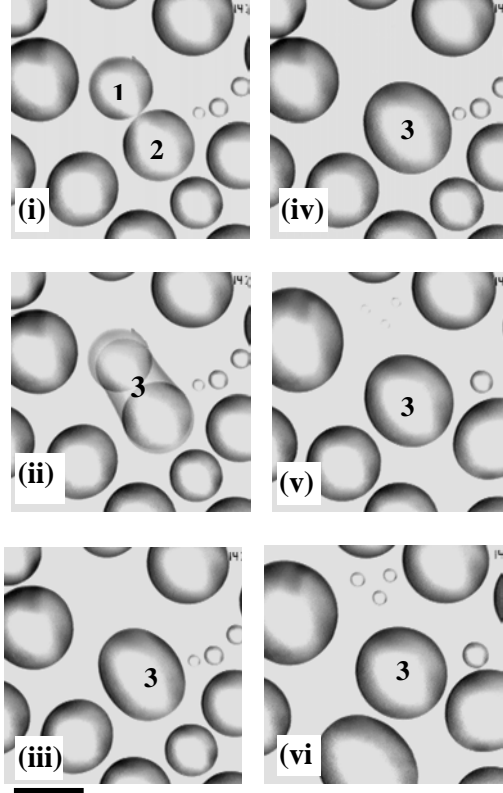can be obtained by estimating the initial (at the beginning of the stage 2) contact angle $\theta_0 = \theta(0)$.

Fig.1. Photo of the coalescence process on Si (LETI) in a condensation chamber. (i) 0.83s (ii) 0.85s; (iii)1.85s; (iv) 11.85s; (v)26.85s; and (vi)51.85s. The bar is of 50μm; The side of each photo corresponds to 172μm.

To estimate this θ_0 angle we assume that during the stage 1, R_y does not change so that the contact line stays pinned. For the estimation purposes it can be assumed that the composite drop at t=0 takes the spheroid shape which is described analytically by Nikolayev and Beysens [1]. By postulating $R_y = 2R_x$ at t = 0, one can obtain a relationship between the composite drop volume Vc, R_y and cosθ. The volume Vc can be found by adding the volumes of two identical spherical cap shaped drops of the volume V, Vc=2V. These drops are assumed to be at equilibrium just before coalescence begins. It means that their contact angle is θ_r. Their base radius R can then be obtained from the expression [9]

$$V = \frac{\pi}{3} R^3 \frac{(1-\cos\theta)(2+\cos\theta)}{(1+\cos\theta)\sin\theta}$$ (4)

Since the points M_1 and M_2 are assumed to be immobile during the first stage, R_y=2R. These equations allow f to be calculated, provided V and θ_r are given. The values are reported in Table II. The value of θ_0 is always markedly different from θ_{eq}, so that the contact angle hysteresis – which is a mean measure of the surface roughness - does not influence much the contact line motion. Eq. 2 can be compared to

$$f \approx \sigma_{lv}\left(\cos\theta_0 - \cos\theta_{eq}\right)$$ (5)

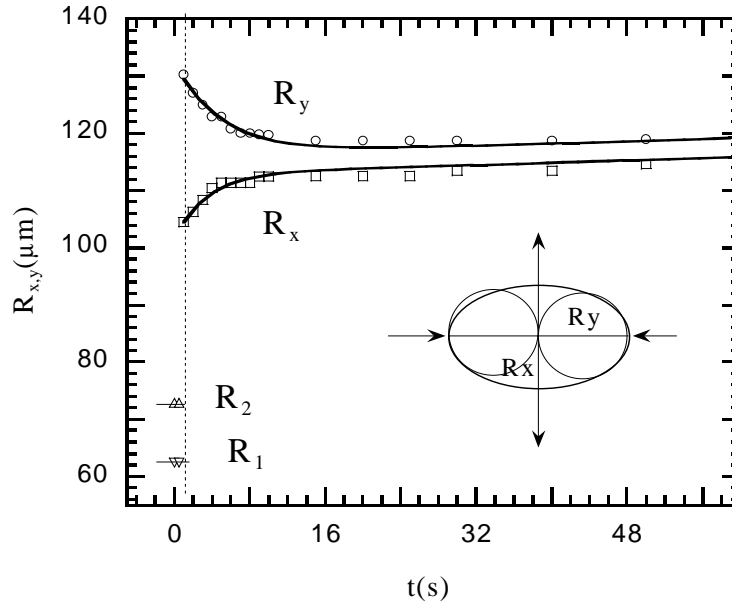where the surface roughness influence is absent.

Fig 2. Time evolution of large radius R_y and small radius R_x of composite drop. The lines are best fits to Eq. (6).

Fig.3 is relaxation time t_c versus equilibrium radius R on log-log scale for silicon substrate. The relaxation time t_c is obtained by fitting relaxation data by an equation of the form

$$R_{x,y}(t) = R_0 \exp\left[\frac{-(t-t_0)}{t_c}\right] + R_1 + A(t-t_0)$$ (6)

5

The first term corresponds to the relaxation of the composite drop, which is dominating in regime 2, the second and third term approximately describes the slow growth due to the condensation which dominates the regime 3. The time of coalescence beginning is t_0. Its experimental value is imposed in the fit. R_0, R_1, A, t_c are the fitting parameters. The relaxation time t_c follows a linear variation with R

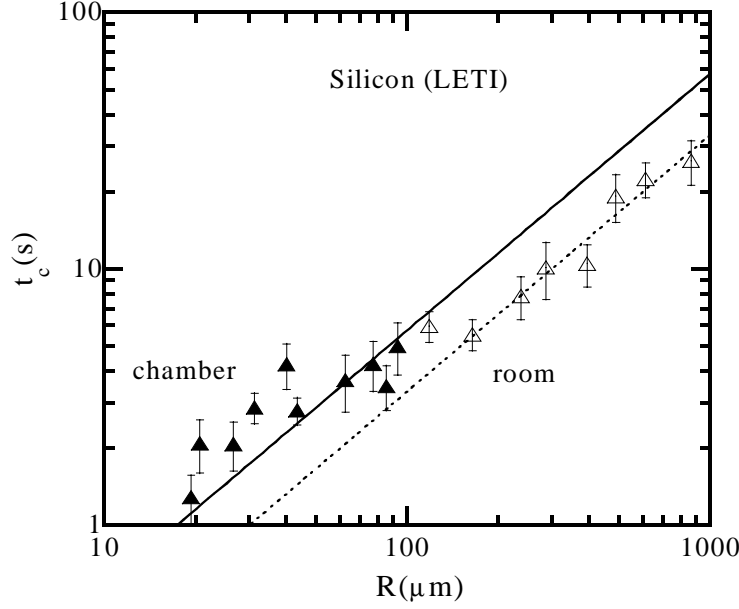$$t_c = \left(\frac{1}{U^*}\right) R \tag{7}$$

as shown in Fig 3.

Fig.3. Relaxation time on Si by condensation in chamber and in room at T=23°C, <Td=18°C, using the syringe imaging device. Lines: fit to Eq. 7; full line U* = (3.0 ± 0.15) 10^{-5} m/s; interrupted line: U* = (1.7 ± 0.16) 10^{-5} m/s. The difference can be attributed to the evolution of the substrate cleanness.

The value of U^* (slope of t_c against R equilibrium graph) characterizes the velocity of the contact line motion. Note that this velocity is not the contact line speed, which obviously varies with time during the relaxation process. The U^* values obtained for silicon and polyethylene substrate are given in table I, together with the treated quartz substrates used by Andrieu et al. It shows that U^* for silicon surface is one order smaller than for polyethylene. The dynamics is faster for larger contact angle (in polyethylene) as the leading capillary force that moves the contact line is larger, which is in good agreement with the predictions of Nikolayev and Beysens [1]. According to them, t_c should vary with θ as:

$$t_c = \frac{1}{K}\frac{\eta}{\sigma}\Phi(\theta) R \tag{8}$$

This defines U^* as

$$U^* = K\frac{\sigma}{\eta}\frac{1}{\Phi(\theta)} \tag{9}$$

with

6

$$\Phi(\theta) = 45 \frac{1 + \cos\ \theta}{(108 + 41\cos\ \theta + 14\cos^2\ \theta + 17\cos^3\ \theta)(1 - \cos\theta)} \tag{10}$$

In Fig.4 we have plotted the values of $U^*/U = K/\Phi(\theta)$ (with $U = \sigma/\eta$, $\sigma = 73$ mN.m^{-1} and $\eta = 10^{-3}$ Pa.s) with respect to θ in a semi-log plot. Both condensation and syringe experiments were performed several times and each data point was obtained by averaging over 15 to 20 measurements. Although the data are scattered, they fit the above θ variation with very small K value. Although the syringe experiments give receding kinetics faster than chamber experiments by one to two order of magnitudes, the kinetics remains many order of magnitude slower than predicted by bulk hydrodynamics. The value of K is still of order 10^{-4}. The scatter of data can be attributed to the different substrate geometrical and/or chemical roughness that locally pin the contact line in a metastable state and thus lead to measure a smaller t_c [1]. The different substrate properties (chemical/geometrical) can not be well controlled which results in to the scattering of data.
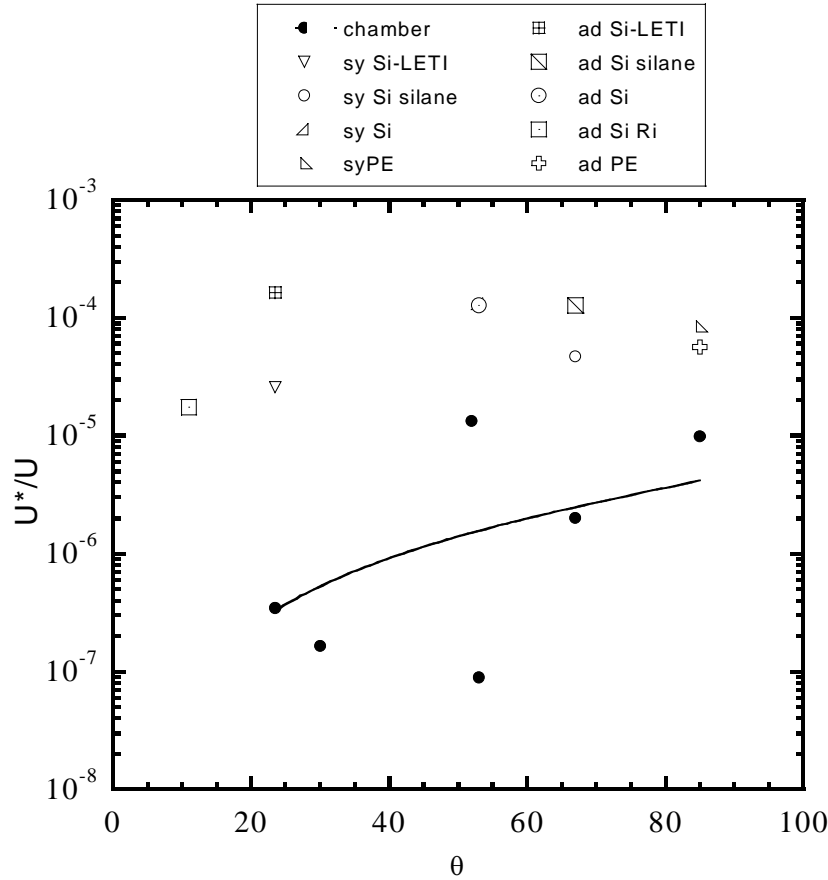

Fig.4. Experimental ratio U^*/U from Table I with respect to θ for different substrates and coalescence methods. Full dots: chamber condensation. Full line: best fit to $K/\Phi(\theta)$, with $K = 2 \times 10^{-6}$. Open signs: syringe experiments. (coalescence, spreading, see symbols).

3.2. Spreading with syringe

Figure 5 is R vs t data for spreading of water drop on silicon surface in syringe experiment. In this experiment drop of known volume is deposited on a flat horizontal substrate surface and the complete process of spreading is recorded with a video camera. Recording is done for the drops of the different size. The relaxation time is obtained by fitting the data by the exponential function. The relaxation time is comparable to the receding experiments with coalescence. It is interesting also to compare the spreading relaxation here and that of Rieutord et al. [10] when they are fitted to the same exponential relaxation. Both data exhibit clearly exponential relaxation, with comparable values of U* = 3.65×10^{-3} m/s and 11.75×10^{-3} m/s (form the fits). It is interesting to estimate the moving force in the advancing-controlled spreading case and compare it to the receding-controlled coalescence case. The volume (V1) of the added drop at the top of the other (V2) can be varied from 1 /4 to 1. The amplitude of the dynamic contact angle is less important and the effect of hysteresis is more pronounced as shown in Table II.
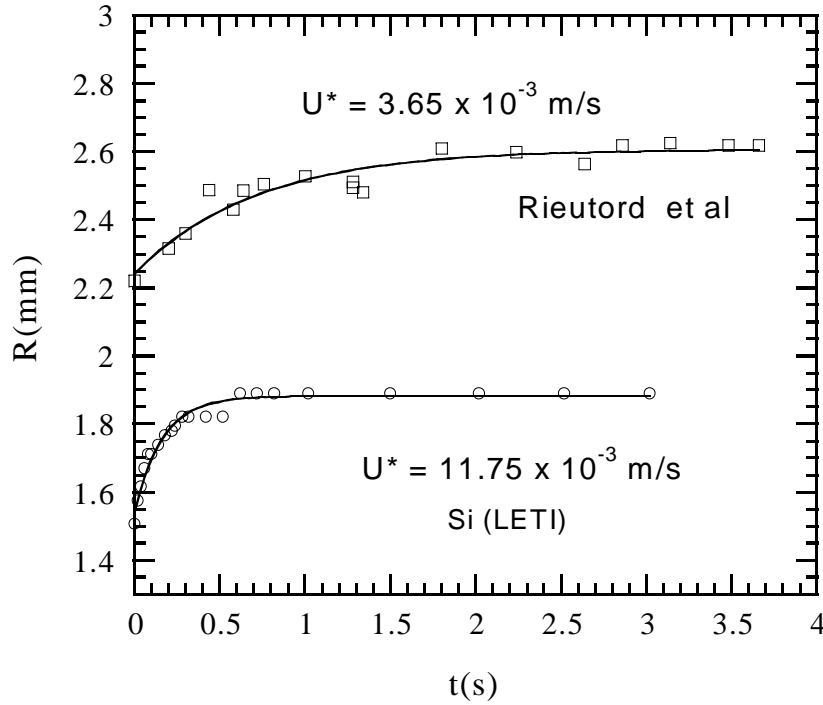

Fig 5. R vs t data for spreading of water drop of comparable size on silicon surface in syringe experiment.

4. CONCLUSION

These experiments show that the dynamics of low viscous sessile drops (spreading, coalescence) is limited by the dissipation in the contact line. This dissipation can lead to relaxation 6 or 7 orders of magnitude lower than expected from bulk dissipation. On experimental grounds, the relaxation is much affected by the contact angle, which results in a decrease of velocity for decreasing angle, due to the decrease

in the capillary leading force. Relaxation is also very affected by the surface roughness, which can soon pin the contact line. A last parameter concerns the initiation of spreading and/or coalescence, which, as syringe deposition, induces strong surface drop oscillations and speeds up relaxation.

It is therefore very difficult to assign a precise value for the ratio, ($K=\eta/\xi$), that can vary between 10^{-4} (syringe deposition) to 10^{-7} (chamber coalescence). Within these limitations, it was, however, not possible to see any difference between spreading and receding (coalescence).

REFERENCES

1. V S. Nikolayev and D. A. Beysens, Phys. Rev. E **65**, 46135 (2002).
2. P.G. de Gennes, Rev. Mod. Phys. **57**, 827 (1985).
3. M. Voué, M .P. Valignat, G. Oshanin, A.M. Cazabat, and J. de Coninck, Langmuir **14**, 5951 (1998).
4. T. D. Blake, C. Decamps, J.De Coninl, M. de Ruijter and M. Voué, Colloids and surfaces A **154**, 5 (1999).
5. T. D. Blake and J. M. Haynes, J. colloid Interface Sci. **30,** 421 (1969).
6. Y. Pomeau, C. R. Acad. Sci. IIb : Mec.,Phys.,Chim., Astron.**238**, 411 (2000).
7. C. Andrieu, D. A. Beysens, V.S. Nikolayev and Y. Pomeau, J. Fluid. Mech. **453**, 427 (2002).
8. Zhao H. and D. Beysens, Langmuir **11**, 627 (1995).
9. M.J. de Ruijter, J. De Coninck and G. Oshanin , Langmuir **15**, 2209 (1999).
10. F. Rieutord, O. Rayssac and H. Moriceau, Phys. Rev. E **62**, 6861 (2000).

Table I. The contact angles and contact line velocities of composite water drop on silicon with various treatment, glass and polyethylene substrate.

substrate	θ_r (deg)	θ_a (deg)	θ_{eq} (deg)	coalescence Chamber Expt. U^*_{chmb} (m/s)	coalescence syringe Expt. U^*_{rec} (m/s)	spreading Syringe Expt (U^*_{sprd} (m/s))
Glass [7]	46	60	53	$(6.5 \pm 0.4) \times 10^{-6}$	---	---
	23	37	30	$(12 \pm 1) \times 10^{-6}$	---	---
Silicon(LETI)	(22 ± 2)	(25 ± 2)	23.5	$(25.07 \pm 1.2) \times 10^{-6}$	$(18.90\pm1.21) \times 10^{-4}$	$(11.94 \pm 0.47) \times 10^{-3}$
Silicon + silane	(55 ± 2)	(79 ± 2)	67	$(1.47 \pm 0.19) \times 10^{-4}$	$(3.42 \pm 0.65) \times 10^{-3}$	$(9.3 \pm 1.6) \times 10^{-3}$
Silicon	(47 ± 2)	(57 ± 2)	52	$(9.74 \pm 0.12) \times 10^{-4}$	$(9.54 \pm 0.7) \times 10^{-3}$	$(9.3 \pm 1.6) \times 10^{-3}$
Silicon [10]	10	12	11	---	---	3.65×10^{-3}
Polyethylene	(80 ± 2)	(90 ± 2)	85	$(7.24 \pm 0.7) \times 10^{-4}$	$(6.15 \pm 0.6) \times 10^{-3}$	$(4.1 \pm 0.9) \times 10^{-3}$

Table II. The initial contact angle calculated from geometry and the capillary force F in case of coalescence. (a) Positive value: no spreading force.

substrate	θ_{eq} (deg)	coalescence			spreading			
		θ_0 (deg) from geometry	$\theta_{eq}=\theta_r$ (deg)	$\sigma_{lv}(\cos\theta_0-\cos\theta_{eq})$ mN/m	θ_0 (deg) from geometry	$\theta_{eq}=\theta_a$ (deg)	$\sigma_{lv}(\cos\theta_0-\cos\theta_{eq})$ mN/m	
							$V_1/V_2=1/4$	$V_1/V_2=1$
	53	29.56	46	12.79	--	--	--	--
Glass [7]	30	15.23	23	3.14	--	--	--	--
Silicon(LETI]	23.5	12.01	22	3.72	28.9	25	-2.3	-13.4
Silicon + silane	67	39.93	55	14.11	76.4	79	3.3[a]	-20.3
Silicon	52	28.88	47	14.13	61.0	57	-4.4	-27.7
Silicon [10]	11	--	--	--	--	--	--	--
Polyethylene	85	56.32	80	27.81	93.5	90	-4.5	-23.8